applied sciences

MDPI

Article

Study on the Influence of Gas Desorption Characteristics of Different Coal Bodies under Hydraulic Permeability Enhancement

Shuyin Ma [1,2,3,4], Qinghua Zhang [3,4], Jianjun Cao [3,4] and Sheng Xue [1,5,*]

[1] School of Safety Science and Engineering, Anhui University of Science and Technology, Huainan 232001, China; 2020100033@aust.edu.cn
[2] State Key Laboratory of Mining Response and Disaster Prevention and Control in Deep Coal Mines, Anhui University of Science and Technology, Huainan 232001, China
[3] China Coal Technology Engineering Group, Chongqing Research Institute, Chongqing 400039, China; zqhcqmky@163.com (Q.Z.); caojianjun206@126.com (J.C.)
[4] State Key Laboratory of the Gas Disaster Detecting, Preventing and Emergency Controlling, Chongqing 400037, China
[5] Joint National-Local Engineering Research Centre for Safe and Precise Coal Mining, Anhui University of Science and Technology, Huainan 232001, China
* Correspondence: sheng.xue@aust.edu.cn

Abstract: To investigate the influence of hydraulic permeability enhancement on the gas desorption and accumulation characteristics of water-bearing coal bodies and deeply implement hydraulic fracturing measures to prevent and control gas disasters in coal seams, isothermal adsorption/desorption tests, low-pressure CO_2 adsorption tests, and X-ray diffraction (XRD) tests were performed on anthracite from Anbao Coal Mine in Guizhou and bituminous coal from Huainan Pan'er Coal Mine. The study results showed that the gas desorption by kinds of water-bearing coal samples (anthracite) and bituminous coal (PE) was evidently promoted by stress. After each stress path, differences were observed between coal samples in gas desorption, which, however, presented similar variation trends. The gas desorption of the AB coal samples was greater than that of PE coal samples, and the increment of the limiting gas desorption by the AB coal samples was greater than that by the PE coal samples. The specific surface area of the AB coal samples was larger than that of the PE coal samples, and they both contained hydrophilic minerals and moisture. It was found through field observation that after hydraulic permeability enhancement acted upon water-bearing coal, the desorbed gas passively migrated under the stress action. When the coal body was free from the hydraulic stress action, gas started flowing back. The study results reveal the influence of hydraulic permeability enhancement on the accumulated gas desorption characteristics of water-bearing coal, and will be of theoretical and practical engineering significance for the prevention and control of gas disasters in coal seams using hydraulic measures.

Keywords: hydraulic permeability enhancement; water-bearing coal body; gas desorption; gas disaster prevention and control

check for updates

Citation: Ma, S.; Zhang, Q.; Cao, J.; Xue, S. Study on the Influence of Gas Desorption Characteristics of Different Coal Bodies under Hydraulic Permeability Enhancement. *Appl. Sci.* **2023**, *13*, 11648. https://doi.org/10.3390/app132111648

Academic Editor: Weifeng Li

Received: 1 October 2023
Revised: 15 October 2023
Accepted: 19 October 2023
Published: 25 October 2023

Copyright: © 2023 by the authors. Licensee MDPI, Basel, Switzerland. This article is an open access article distributed under the terms and conditions of the Creative Commons Attribution (CC BY) license (https://creativecommons.org/licenses/by/4.0/).

1. Introduction

Underground mining, including underground coal mining, is accompanied by the danger of arising emergencies and fire hazards that pose a threat to the life safety of miners [1,2]. The development of mining enterprises implies the complication of mining–geological conditions: an increase in the depth of mining operations and natural gas content of coal seams, the depletion of highly productive reserves, etc. Gas disasters have been affecting the safety production of coal mines for many years. Gas migration, extraction, and coal gas outburst are closely related to gas desorption and permeability characteristics, so studying the gas desorption characteristics in the process of gas control will be of certain practical significance. The gas desorption characteristics in coal seams are affected by such

factors as the coal structure, ground stress, gas pressure, and moisture [3,4]. The factors affecting the gas desorption state of coal bodies under complex conditions have been widely investigated by many Chinese and foreign experts and professors, and abundant results have been achieved [5–16].

At present, the research on the influencing factors of gas desorption and diffusion in underground coal bodies mainly focuses on temperature [17–20], moisture [21], coal quality [22], gas pressure [23,24], failure type [25] and so on. However, the influence of underground stress on the desorption characteristics of coal bodies have been investigated less. Lv X F et al. [26] obtained the relationship between pore pressure and desorption amount through simulation. Wang D K et al. [27] applied axial pressure to raw coal and figured out the relationship between gas desorption and axial pressure before and after peak intensity. Jia Y N et al. [28] experimentally found that there was a "V-shaped" relationship between the amount of gas desorption by loaded raw coal and stress.

Considering the difficulties in coal gas desorption, poor permeability, and poor drainage effect faced in gas extraction at present, and in order to improve the stress disequilibrium (stress generates a significant influence on the gas desorption–diffusion process inside the coal body) induced by underground mining activities, the underground hydraulic permeability enhancement process was implemented to effectively enhance the permeability of the coal body. Furthermore, the influencing mechanism of hydraulic permeability enhancement stress on the desorption characteristics of water-bearing coal bodies was expounded. With bituminous coal from Huainan Pan'er Coal Mine and anthracite from Anbao Coal Mine in Guizhou as the study object, the high-pressure hydraulic permeability enhancement stress state borne by the coal body was approximately simulated under different stress action modes, followed by the isothermal desorption tests of coal samples. In this way, the gas emission phenomenon after permeability enhancement was accurately figured out, and, meanwhile, this laid a theoretical foundation for gas disaster control.

2. Test

2.1. Preparation of Coal Samples

In order to meet the requirements of this test, coal samples with different degrees of metamorphism were taken as the test objects, namely, bituminous coal (PE) in Huainan Pan'er Coal Mine and anthracite (AB) in Guizhou Anbao Coal Mine. Among them, the raw coal sample used in this test was taken from 12,023 fully mechanized mining faces of 3 coal seams in Panser Coal Mine, Huainan, with a burial depth of 490 m and coal type of bituminous coal. A total of 10,103 fully mechanized mining faces of the main coal seam in Anbao Coal Mine, Guizhou Province, with a burial depth of 440 m, consist of anthracite coal.

The coal samples needed for the test were collected from the coal mine underground and directly sealed and transported to the laboratory for sample preparation before the test. Some of coal samples were crushed and sieved into 40–60 mesh pulverized coal for low-pressure CO_2 adsorption test. Some were sieved into 200-mesh pulverized coal for XRD tests. The remaining raw coal was crushed, the particle size of 0.2~0.5 mm of coal powder was screened, and an appropriate amount of distilled water was added to the coal powder and stirred evenly. The stirred coal powder was loaded into the sample making mold, and the Φ50 mm × 100 mm standard specimen was made by a press under the loading condition of 150 kN for the triaxial isothermal coal rock adsorption/desorption tests. The remaining two kinds of coal blocks were fabricated into Φ50 mm × 100 mm standard samples or triaxial isothermal coal-rock adsorption/desorption tests. The coal samples are exhibited in Figure 1.

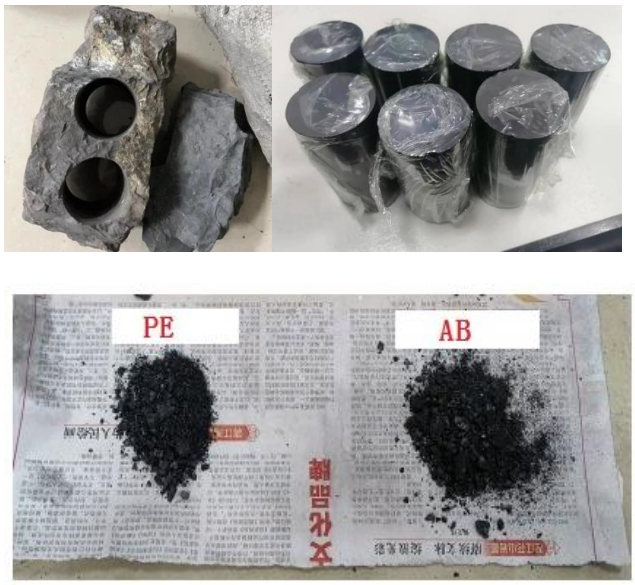


Figure 1. Preparation of coal samples.

According to the industrial analysis of coal samples provided by Huainan Pan'er Coal Mine and Guizhou Anbao Coal Mine, the basic parameters of the two types of coal samples are listed in Table 1.

Table 1. Industrial analysis results of coal samples.

Coal Sample	M_{ad}/%	A_{ad}/%	V_{daf}/%	F/%	Gas Adsorption Constant $a/(cm^3 \cdot g^{-1})$	b/MPa^{-1}
PE	2.54	38.34	42.98	4.82	17.9779	1.1547
AB	2.77	8.03	6.47	8.22	39.842	0.627

According to the industrial analysis parameters of the coal samples provided, there is a large gap between the parameters of AB and PE coal samples. Among them, the adsorption constant of AB coal sample is higher than that of PE coal sample, indicating that the gas adsorption capacity of AB coal sample is strong, and the gas is not prone to desorption in the natural state.

2.2. Isothermal Adsorption and Desorption Tests of Water-Bearing Coal under Stress Action

In order to explore the gas desorption characteristics of different water-bearing coal bodies, a triaxial coal rock adsorption/desorption seepage testing apparatus was adopted in this test. This testing apparatus, which was an improved device, was convenient for the isothermal adsorption/desorption test of water-bearing coal bodies under various stress paths. The coal samples were given the adsorption equilibrium in the stress chamber under confining pressure of 3 MPa, gas adsorption was performed under adsorption equilibrium pressure of 2 MPa, and water-bearing coal samples were subjected to gas desorption under different axial stresses (0, 4, 8, 12, and 16 MPa). As shown in Figure 2, this testing apparatus was composed of a vacuum pump, a methane tank, a temperature control and pressure adjustment device, a stress chamber, a constant-temperature device, and a gas metering and analysis system. The test flow is as follows:

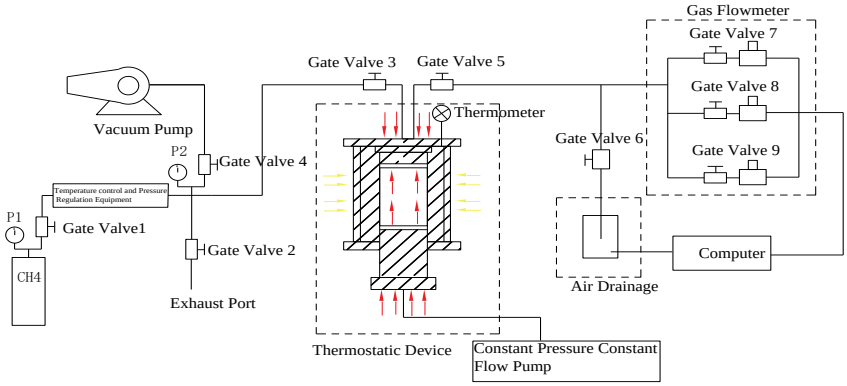


Figure 2. Experimental equipment.

(1) The Φ50 mm × 100 mm samples were fabricated at specific moisture content [29,30], and the moisture content in both the first group (PE) and the second group (AB) was 2.65%.

(2) The valve of the whole system was temporarily closed, and the samples were fixed in the stress chamber under confining pressure of 3 MPa. The vacuum pump was started and valves 4 and 3 were opened for vacuum degassing.

(3) After degassing, the temperature-controlling and pressure-regulating device was used to control the gas temperature and pressurize the gas, valve 1 was opened while valve 4 was closed so that gas was charged into the temperature-controlling and pressure-regulating device, and the temperature was regulated to 30 °C. Meanwhile, the temperature in the stress chamber was kept constant at 30 °C, the temperature-controlling and pressure-regulating device and valve 3 were opened to charge gas into the stress chamber, and the change in the gas pressure was observed in the process of gas adsorption by the coal samples.

(4) When the pressure gauge reading of the stress chamber was stable, namely, gas adsorption was completed, the set axial pressure was applied to the coal samples, and valve 5 was opened to discharge the free gas in the stress chamber. When the pressure reading of the observation instrument was 0, it was considered identical with atmospheric pressure. In this case, the gas metering device was started to perform the isothermal desorption test of water-bearing gas coal bodies under different stress paths, and the gas amount was recorded.

3. Test Results and Analysis

3.1. Analysis of Low-Pressure CO_2 Adsorption Test Results

For coal samples, the micropore specific surface area is the dominant factor of gas adsorption capacity in coal [29,31]. In order to study the gas adsorption capacity of PE coal samples and AB coal samples, the two types of coal samples were subjected to low-pressure CO_2 adsorption tests from the angle of their micropore structural characteristics. [32].

As shown in Figure 3, the pore size distribution of AB and PE coal samples was obtained through tests. It could be seen that AB coal samples had the maximum peak at 0.4–0.7 nm and PE coal samples at 0.4–0.6 nm, and AB coal samples showed several small peaks at 0.7–1.2 nm and PE coal samples at 0.7–0.9 nm, indicating the appearance of many pores in this range. Meanwhile, it was known that AB coal samples were anthracite with relatively developed micropores, mainly because anthracite had a high degree of coalification and metamorphism, while PE coal samples were bituminous coal with a low degree of metamorphism and a low level of micropore development. The development of micropores was positively correlated with the specific surface area, and the larger the specific surface area, the stronger the gas adsorption, directly proving that the maximum gas adsorption capacity (39.842 $cm^3 \cdot g^{-1}$) of AB coal samples was greater than that (17.9779 $cm^3 \cdot g^{-1}$) of PE coal samples.

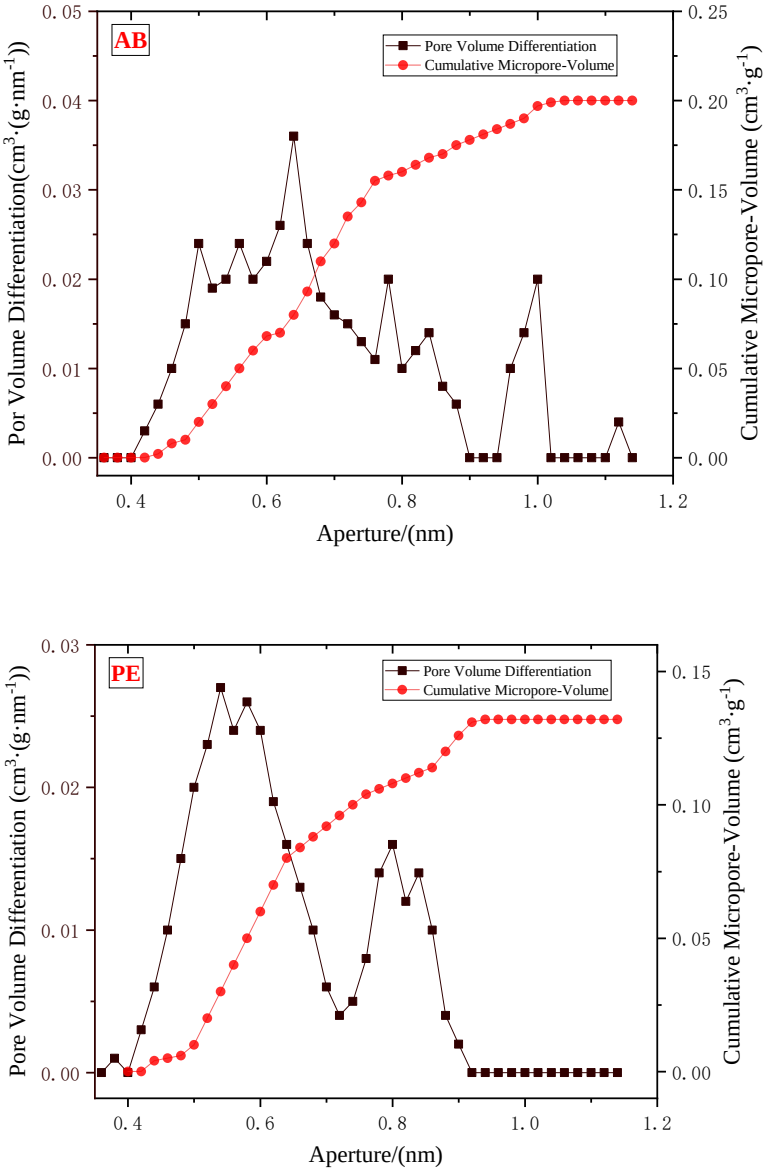


Figure 3. Micropore size distribution and cumulative micropore volume of AB and PE coal samples.

3.2. Analysis of XRD Test Results

Figure 4 shows the XRD patterns of the two types of coal samples, in which the X-ray diffraction peak was positively correlated with the amount of minerals, and the higher the diffraction peak, the higher the corresponding mineral content. As can be seen from the figure, the main mineral components of AB coal samples were muscovite, gypsum, and quartz, among which muscovite had four peaks, gypsum had two peaks, and quartz had one peak. The main mineral components of PE coal samples were kaolinite and montmorillonite, in which kaolinite had five peaks and montmorillonite had one peak. The higher the diffraction peak, the more mineral components there were. Gypsum and quartz minerals in AB coal samples were hydrophilic to some extent, and montmorillonite minerals in PE coal samples were also hydrophilic, but kaolinite minerals showed weak hydrophilicity. Combined with the test results, the minerals in coal had an important influence on the wettability of coal samples.

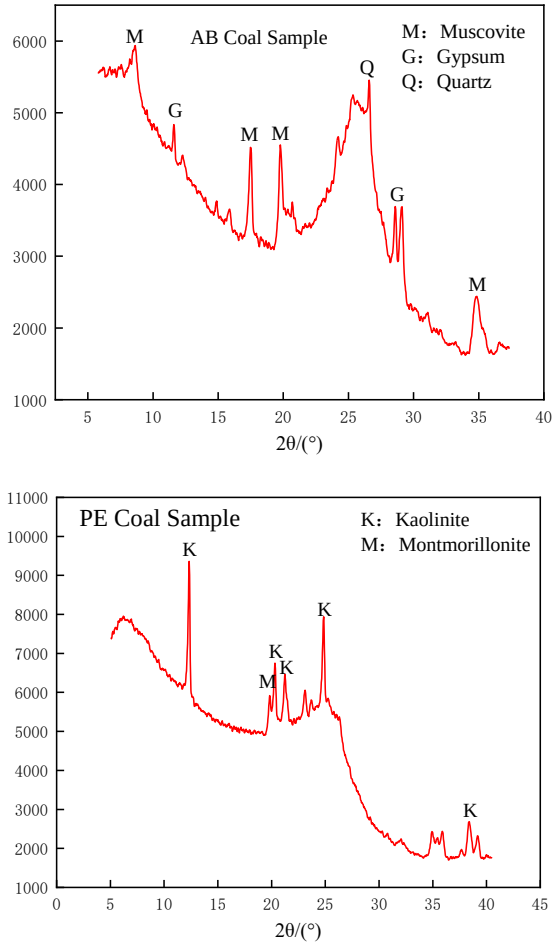


Figure 4. XRD patterns of AB and PE coal samples.

4. Gas Desorption Law of Different Water-Bearing Coal Bodies under Various Stress Paths

Under the influence of hydraulic fracturing and permeability enhancement stress, water- and gas-bearing coal bodies were subjected to different stress loads, which would significantly affect the gas adsorption capacity of coal bodies and also lead to the change in the adsorption–desorption state after the coal body was subjected to the action of different stresses. To explore the gas desorption and emission laws after different water-bearing coal bodies bore the action of various stress paths, therefore, the gas desorption of different water-bearing coal bodies was analyzed by combining the triaxial coal rock adsorption/desorption seepage testing apparatus and the stated testing method.

4.1. Influencing Analysis of Gas Desorption by Water-Bearing Coal under Various Stress Paths

The change in gas desorption by water-bearing coal under different stress conditions could be characterized using the accumulated gas desorption during the test. Specifically, the time-dependent variation trend of gas desorption was characterized through the Langmuir-type relational expression, and the accumulated gas desorption by different water-bearing coal bodies under various stress paths was further analyzed [33,34].

$$Q_t = \frac{AB\sqrt{t}}{1 + B\sqrt{t}} \quad (1)$$

where Q is the accumulated gas desorption at time t, mL/g; t is desorption time, s; A represents the limiting gas desorption, mL/g; and B is the desorption rate constant.

Combining the test, the accumulated gas desorption of different water-bearing coal bodies under different stress paths was finally measured and fitted as per Formula (1). Then, the limiting accumulated gas desorption of AB and PE coal samples under different test conditions was acquired, and the gas desorption curves of different water-bearing coal bodies and the change curves of their limiting accumulated gas desorption under various stress paths were plotted as shown in Figures 5–8.

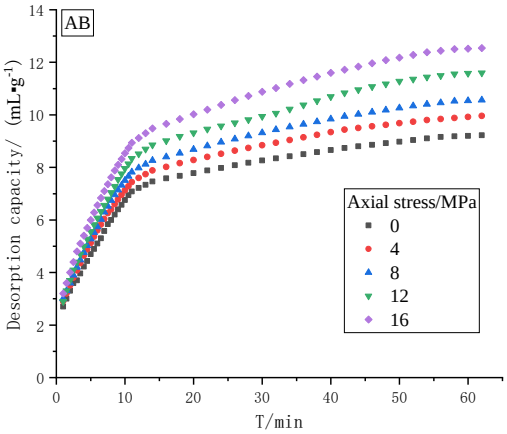


Figure 5. Gas desorption curves of AB coal samples with moisture content of 2.65% under various stress path states.

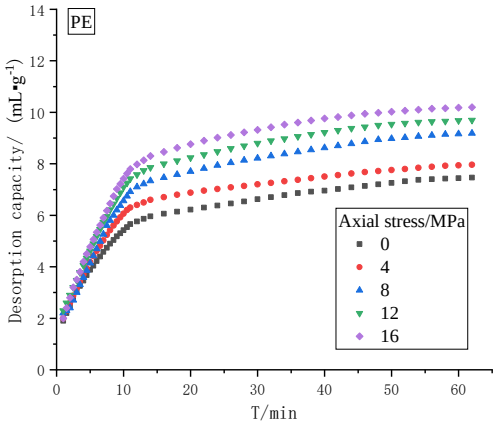


Figure 6. Gas desorption curves of PE coal samples with moisture content of 2.65% under various stress path states.

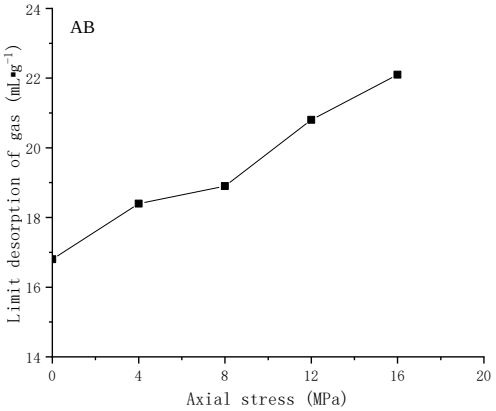


Figure 7. Changes in limiting gas desorption of AB coal samples with moisture content of 2.65% under various stress path states.

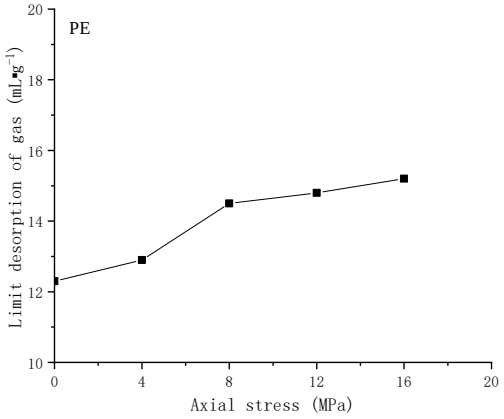


Figure 8. Changes in limiting gas desorption of PE coal samples with moisture content of 2.65% under various stress path states.

By analyzing Figures 5–8, it can be seen that: (1) AB and PE coal samples were subjected to different stress paths under a certain water-bearing state, and the corresponding gas desorption process was also different. Taking 12 min as the time node in the curve change of the figures, within 0–12 min in the initial stage, the stress borne by the two types of coal samples gradually increased and the gas desorption grew rapidly, but an overlapping gas desorption was observed in this initial stage. According to the gas desorption curves, it could be observed that the total gas desorption by coal samples was in direct proportion to the stress increase at the same time node. (2) AB and PE coal samples experienced the action of various stress paths under the water-bearing state, and they differed in gas desorption after each stress path exerted its action, but the variation trend of gas desorption was similar, where the gas desorption by AB coal samples was greater than that by PE coal samples under all stress paths.

It can be observed from Figures 7 and 8 that when the stress borne by AB and PE water-bearing coal samples rose from 0 MPa to 16 MPa, the fitted limiting desorption of AB coal samples was about 16.931–22.131 mL/g, with an increase of 5.2 mL/g, and that of PE coal samples' fitted limiting desorption was about 12.331–15.223 mL/g, increasing by 2.892 mL/g. Axial stress exerted an obvious promoting effect on the gas desorption of two types of coal samples, but the effect varied. The increment of limiting desorption by AB coal samples was greater than that by PE coal samples.

4.2. Influencing Analysis of Stress on Gas Desorption and Emission of Water-Bearing Coal Bodies

A multi-stage pore system was observed in the coal body, in which anthracite was characterized by a high degree of coalification and metamorphism, a large specific surface area, and strong gas adsorption capacity. The degree of coalification and metamorphism of bituminous coal was inferior to that of anthracite, accompanied by a smaller specific surface area than anthracite and relatively weaker gas adsorption capacity. Influenced by the stress action, the particle skeleton structure and pore volume of two types of coal were compressed, and the original gas adsorption equilibrium was broken. Moreover, the water and gas molecules in coal bodies competed for adsorption and desorption, but under stress action, the gas adsorption capacity was weakened, and a significant number of water molecules infiltrated into the pore diffusion system to displace gas molecules in a specific stage. Because the pore volume and coal skeleton structure were compressed, the pore diffusion system and seepage system of water molecules were indirectly connected, resulting in differences in accumulated gas desorption and emission in this zone. As shown in Figure 9, the pore system channel was reduced due to the stress action on the coal body, which directly increased the gas migration resistance. In the figure (water molecules are blue and gas molecules are colorless), A is the channel diameter of the pore system without stress (solid line) and A1 is the channel diameter after the stress action (dotted line) [35]. In response to the force acting on the coal skeleton structure, the reduction in

gas migration channels directly increased the pore pressure, which enlarged the pressure difference between gas channels and increased the gas accumulation.

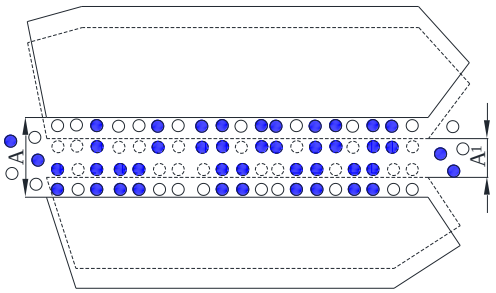


Figure 9. Changes in gas fracture channels under stress action.

5. Field Gas Measurement and Analysis

In order to measure the influence of hydraulic permeability enhancement stress on gas desorption on site, hydraulic permeability enhancement process tests were performed in geological structure-free areas with steady coal seam occurrence in the haulage roadway on the working face of Guizhou Anbao Coal Mine and Huainan Pan'er Coal Mine. Fracturing boreholes and observation holes (1#–5#) were constructed for each, respectively, where the fracturing boreholes in the two test areas were 30 m from the observation drill hole 1#, and the single-hole (1#–5#) pure gas extraction was investigated, as shown in Figure 10.

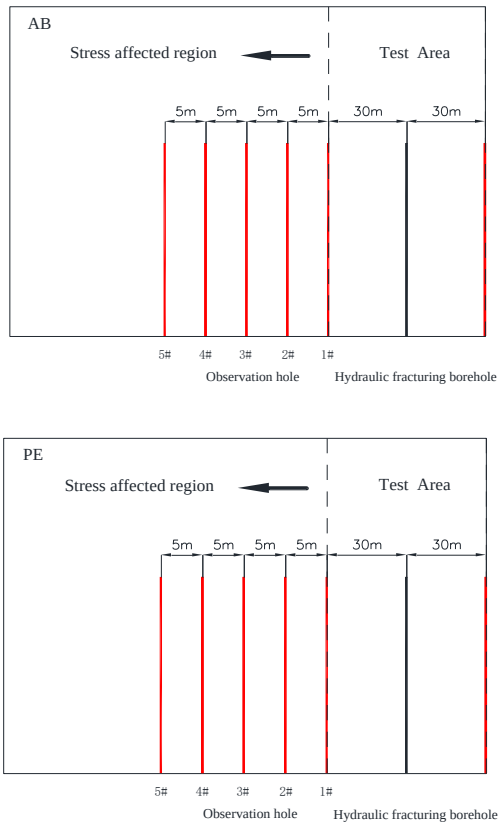


Figure 10. Layout plan of drill holes in two test areas (The red holes are observation holes).

For this test step, in both test areas, observation holes were drilled before the hydraulic permeability enhancement process (observation holes were used for gas extraction and hole drilling simultaneously) was implemented, with a spacing of 5 m. In the testing process, the pressure range of hydraulic permeability enhancement was 0–32 MPa, and

after pressurization was initiated, the pressure was stabilized at 28–31 MPa. After the test was ended, the single-hole water injection was 156.4–188.6 m^3.

Combining the previous hydraulic permeability enhancement tests in the test areas of Anbao Coal Mine and Pan'er Coal Mine, the radius of effective fracturing influence was 26.5 and 23.2 m, respectively, and the test areas belonged to the same geological unit and the same coal seam as the previous test areas. Therefore, the radius of effective fracturing influence was set to 30 m during hydraulic permeability enhancement in order to approach the test effect and ensure the reasonability of investigation results, and only the peripheral affected zone subjected to the action of hydraulic permeability enhancement beyond this radius distance was included in the investigation. Hereby, the gas extraction in this peripheral affected zone of stress action could be analyzed.

Analysis of Pure Gas Extraction in Stress-Affected Zone

In the stress-affected peripheral zone, the changes in pure gas extraction from observation holes (1#–5#) during the implementation of the hydraulic permeability enhancement process and within 15 d of the completion of the process are displayed in Figure 11.

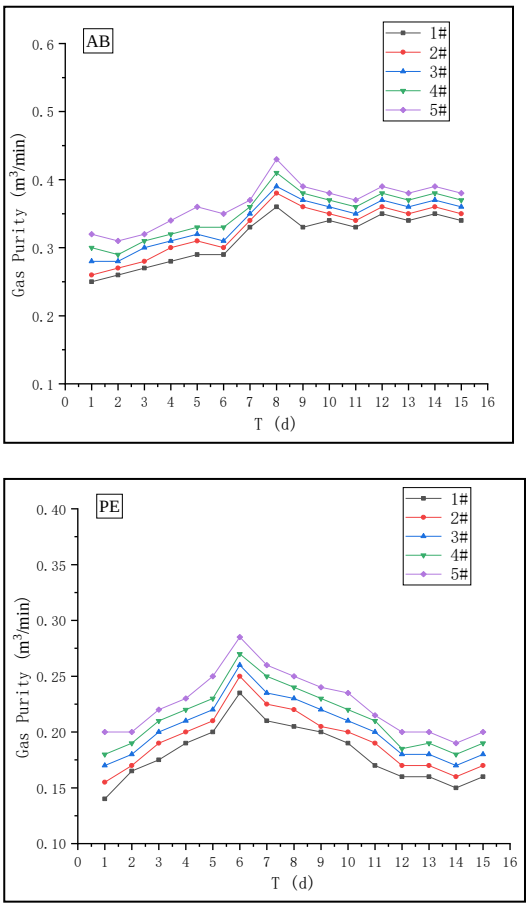


Figure 11. Variation curves of pure gas extraction in stress-affected peripheral zone.

The pure gas extraction from observation holes (1#–5#) in the test area of Anbao Coal Mine was 0.25–0.43 m^3/min, and that in the test area of Pan'er Coal Mine was 0.14–0.28 m^3/min.

During the hydraulic permeability enhancement test, the continuous stress action affected the coal skeleton structure in the test area, narrowed the gas migration channel in the pore system, and enlarged the pressure difference between the two ends of the gas channel. However, coal contained a certain amount of hydrophilic minerals, so it contained water, and the desorption of water-bearing coal was evidently promoted by the stress action,

so a large amount of desorbed gas passively migrated under the continuous stress action. With the attenuation of the stress action, the passive gas migration rate was slowed down, and the gas migration was stopped temporarily, where the gas pressure and gas content reached the maximum value. After the hydraulic permeability enhancement process was ended, the coal body was no longer subjected to the hydraulic stress action. Subsequently, the temporary gas migration stopping state was relieved, the gas migration channel size in the pore system of the coal body was recovered, the pressure difference between two ends of the gas channel was eliminated, and gas started flowing back. It could be seen from the investigation index of field pure gas extraction that peak pure gas extraction appeared in all observation holes for AB coal in the test area of Anbao Coal Mine after 8 d and appeared in the test area of Pan'er Coal Mine after 6 d.

6. Conclusions

(1) Two types of water-bearing coal samples, anthracite (AB) and bituminous coal (PE), can promote gas desorption to some extent, but the effect of each is different. The gas desorption by AB coal samples is greater than that by PE coal samples, and the increment of the limiting desorption by AB coal samples is greater than that by PE coal samples.

(2) The specific surface area of AB coal samples is larger than that of PE coal samples, and the larger the specific surface area of coal, the stronger the gas adsorption, and both AB and PE coal samples contain hydrophilic minerals and a certain amount of moisture.

(3) The stress acts on the water-bearing coal body, and the desorbed gas migrates passively under the stress action. With the attenuation of the stress action, the gas migration stops temporarily, and when the coal body is not affected by the hydraulic driving stress, the gas begins to flow back.

Author Contributions: Methodology, J.C.; Formal analysis, S.X.; Investigation, Q.Z. and J.C.; Resources, Q.Z.; Data curation, S.M. and S.X.; Writing—original draft, S.M.; Project administration, S.X. All authors have read and agreed to the published version of the manuscript.

Funding: This research is supported by the Open Research fund of the Joint National-Local Engineering Research Centre for Safe and Precise Coal Mining (EC2021018); Study on mechanism of rock breaking and hole formation by external rotary multi-jet jet and drill bit structure parameters (cstc2021jcyj-msxmX0564).

Institutional Review Board Statement: Not applicable.

Informed Consent Statement: Not applicable.

Data Availability Statement: The data, figures, and tables used to support the findings of this study are included in the article.

Acknowledgments: The authors would like to show sincere thanks to the technicians who have contributed to this research.

Conflicts of Interest: The authors declare no conflict of interest.

References

1. Miao, D.; Lv, Y.; Yu, K.; Liu, L.; Jiang, J. Research on coal mine hidden danger analysis and risk early warning technology based on data mining in China. *Process. Saf. Environ. Prot.* **2023**, *171*, 1–17. [CrossRef]
2. Bosikov, I.I.; Martyushev, N.V.; Klyuev, R.V.; Savchenko, I.A.; Kukartsev, V.V.; Kukartsev, V.A.; Tynchenko, Y.A. Modeling and Complex Analysis of the Topology Parameters of Ventilation Networks When Ensuring Fire Safety While Developing Coal and Gas Deposits. *Fire* **2023**, *6*, 95. [CrossRef]
3. Zhang, Z.; Liang, W. Experimental study about the effect of adsorbed methane on coal permeabil-ity. *J. Taiyuan Univ. Technol.* **2013**, *44*, 356–360.
4. Rong, T.; Zhou, H.; Wang, L.; Ren, W.; Wang, Z.; Su, T. Study on coal permeability model in front of working face under the influence of mining disturbance and temperature coupling. *Rock Soil Mech.* **2019**, *40*, 4289–4298.
5. Jiang, D.Y.; Yuan, X.; Chen, J.; Jiang, X.; Fan, J.Y.; Ren, S.; Li, L. Effect of adsorptional gases on permeability of outburst coal. *J. China Coal Soc.* **2015**, *40*, 2091–2096.
6. Peng, S.J.; Xu, J.; Yang, H.W.; Liu, D. Experimental study on the influence mechanism of gas seepage on coal and gas outburst disaster. *Saf. Sci.* **2012**, *50*, 816–821. [CrossRef]

7. Soloviev, V.A.; Ginsburg, G.D. Water segregation in the course of gas hydrate formation and accumulation in submarine gas-seepage fields. *Mar. Geol.* **1997**, *137*, 59–68. [CrossRef]
8. Cheng, Q.Y.; Huang, B.X.; Li, Z.H. Evolution law of the structure and permeability for coal under solid-liquid coupling. *J. Min. Saf. Eng.* **2012**, *29*, 400–406.
9. Yin, G.; Huang, Q.X.; Zhang, D.M.; Wang, D. Test study of gas seepage characteristics of gas-bearing coal specimen during process of deformation and failure in geostress field. *Chin. J. Rock Mech. Eng.* **2010**, *29*, 336–343.
10. Xiao, X.C.; Pan, Y.S.; Lv, X.F.; Luo, H.; Li, Z.H. Experimental research on gas flow law of containing water coal specimens in deformation and fracture process. *J. China Coal Soc.* **2012**, *37* (Suppl. 1), 115–119.
11. Yin, G.; Li, X.; Zhao, H.; Li, X.; Jing, X. Experimental study of effect of gas pressure on gas seep-age of outburst coal. *Chin. J. Rock Mech. Eng.* **2009**, *28*, 697–702.
12. Cao, S.; Guo, P.; Li, Y.; Bai, Y.J.; Liu, Y.B.; Xu, J. Effect of gas pressure on gas seepage of outburst coal. *J. China Coal Soc.* **2010**, *35*, 595–599.
13. Liu, R.; Yan, J.; Li, J. Experimental study on effect of coal temperature to gas permeability. *Coal Technol.* **2010**, *29*, 71–73.
14. Gao, J.; Feng, M.; Yang, W. Research on distribution law of frozen temperature field of fractured rock mass with groundwater seepage. *J. Min. Saf. Eng.* **2013**, *30*, 68–73.
15. Wang, D.; Liu, J.; Yin, G.; Wei, X. Test study of creep properties of gas-bearing coal specimens under triaxial compression. *Chin. J. Rock Mech. Eng.* **2010**, *29*, 349–357.
16. Liang, B.; Gao, H.M.; Lan, Y.W. Theoretical analysis and experimental study on relation between rock permeability and temperature. *Chin. J. Rock Mech. Eng.* **2005**, *24*, 2009–2012.
17. Iu, Y.W.; Wei, J.P.; He, Z.G.; Liu, M.J. Influence rules and mechanisms of temperature on dynamic process of gas diffusion from coal particles. *J. China Coal Soc.* **2013**, *38*, 100–105.
18. Liu, Y.; Han, G.; Wang, W.; Huo, Z.; Meng, T. Evolution mechanism of fracture structure of loaded coal under different unloading rates. *J. China Coal Soc.* **2020**, *45*, 3806–3816.
19. Hao, J.F.; Liang, B.; Sun, W.J.; Li, Q.Q.; Dong, P.C. Gassy coal thermal-hydraulic-mechanicalcoupling model and nu- merical simulation consideringadsorption/desorption thermal effect. *J. Min. Saf. Eng.* **2020**, *37*, 1282–1290.
20. Li, B.B.; Wang, B.; Yang, K.; Li, J.H.; Ren, C.H.; Xu, J. Coal seepage mechanism effected by stress and temperature. *J. China Univ. Min. Technol.* **2020**, *49*, 844–855.
21. Chen, X.; Cheng, Y.; Wang, L. Experimental study on the inhibition of injection water to the gas desorption of coal. *J. Min. Saf. Eng.* **2013**, *30*, 296–301.
22. Li, Z.Q.; Liu, Y.; Xu, Y.P.; Song, D.Y. Gas diffusion mechanism in multi-scale pores of coal particles and new diffusion model of dynamic diffusion coefficient. *J. China Coal Soc.* **2016**, *41*, 633–643.
23. Nie, B.; Yang, T.; Li, X.; Li, L.; Lu, H. Research on diffusion of methane in coal particles. *J. China Univ. Min. Technol.* **2013**, *42*, 975–981.
24. Peng, S.J.; Yang, W.J.; Zhou, B.; Xu, J.; Cheng, L.; Yang, X. Study on the evolution law of gas pressure in the process of coal and gas outburst under true triaxial stresses. *Chin. J. Rock Mech. Eng.* **2020**, *39*, 1762–1772.
25. Li, Y. *Research on the Methane Adsorption/Desorption/Diffusion Characteristics of Tectonic Coal*; Henan Polytechnic University: Jiaozuo, China, 2015; Volume 47.
26. Lü, X.F.; Pan, Y.S.; Liu, J.J.; Tang, J.P.; Di, J.Z. Experimental study of effect of pore pressure on desorption deformation of coal matrix. *Rock Soil Mech.* **2013**, *1*, 3447–3451.
27. Dengke, W.A.; Honglei, W.A.; Banghua, Y.A.; Zhihui, W.E.; Yannan, J.I. Experimental investigation of gas desorption law of loaded raw coal. *Coal Geol. Explor.* **2016**, *44*, 10–13.
28. Jia, Y.; Wen, Z.; Yao, B. Experiment of the desorption law of loaded gas-filled raw coal. *Coal Geol. Explor.* **2014**, *42*, 21–30.
29. Wei, J.; Wang, H.; Si, L.; Xi, Y. Characteristics of coal-water solid-liquid contact in gas atmosphere. *J. China Coal Soc.* **2022**, *47*, 323–332.
30. Cheng, Y.; Hu, B. Main occurrence form of methane in coal: Micropore filling. *J. China Coal Soc.* **2021**, *46*, 2933–2948.
31. Wei, J.; Wen, Z.; Yuan, Y.; Wang, Q.; Si, L. Study on influence of stress on desorption characteristics of coal containing gas. *Coal Sci. Technol.* **2021**, *49*, 35–43.
32. Zhang, J.; Li, H.; Liu, Y. Micro-wetting characteristics of coal dust in Pingdingshan mining area. *J. China Coal Soc.* **2021**, *46*, 812–825.
33. Qin, Y.; Wang, Y.; Yang, X.; Liu, W.; Luo, W. Experimental study on dynamie gas adsorption. *Int. J. Min. Sci. Technol.* **2012**, *22*, 761–765. [CrossRef]
34. Zhang, S.; Liu, Y.; Meng, T. Experimental study on influence of water with different salinity on methane desorption per- formance of coal seam. *Coal Sci. Technol.* **2021**, *49*, 110–117.
35. Xie, H.; Gao, F.; Ju, Y. Research and development of rock mechanics in deep ground engineering. *Chin. J. Rock Mech. Eng.* **2015**, *34*, 2161–2178.

Disclaimer/Publisher's Note: The statements, opinions and data contained in all publications are solely those of the individual author(s) and contributor(s) and not of MDPI and/or the editor(s). MDPI and/or the editor(s) disclaim responsibility for any injury to people or property resulting from any ideas, methods, instructions or products referred to in the content.